Kinetic theoretical approach to turbulence in variable-density incompressible, statistically inhomogeneous fluids

G. Hazak,[1] Y. Elbaz,[1] S. Zalesak,[2] N. Wygoda,[1] and A. J. Schmitt[2]
[1]*Physics Department, Nuclear Research Center, Negev, Beer Sheva, Israel*
[2]*Plasma Physics Division, Naval Research Laboratory, Washington, DC 20375, USA*
(Received 22 June 2009; revised manuscript received 22 December 2009; published 26 February 2010)

The kinetic theory is developed for the mass mixing of two incompressible immiscible fluids due to Rayleigh-Taylor instability (as an example for turbulence in variable-density statistically inhomogeneous incompressible fluids). An expression is derived for the fine grain force in terms of the mass-density and velocity fields. This expression enables the conversion of the Navier-Stokes equation into an exact explicit conservation equation in phase space. The equation is a generalization, to the variable-density case, of the Lundgren equation [T. S. Lundgren, Phys. Fluids **10**, 969 (1967)]. The conserved quantity is the fine grain density-velocity distribution (FGDVD). The fine grain mass-density and fluid velocity fields are the two lowest moments of the FGDVD. The joint density-velocity probability density function (DVPDF) is the ensemble average of the FGDVD. Using detailed numerical solutions of the Navier-Stokes equation, it is found that the correlation between the acceleration and the FGDVD is weak. This result identifies a small parameter which enables the derivation, by controlled approximations, of closed equations for the DVPDFs. The lowest order yields the mean-field approximation. It is shown by a numerical solution of the closed kinetic equation in the mean-field approximation that it properly describes the time evolution of the system for periods shorter than the relaxation time. Closure schemes beyond the mean field are discussed.

DOI: 10.1103/PhysRevE.81.026314 PACS number(s): 47.20.Ma, 47.27.eb, 47.51.+a

I. INTRODUCTION

The Rayleigh-Taylor instability (RTI) occurs when a light fluid supports a heavier one against gravity or pushes it with a constant acceleration [1–3]. The phenomenon occurs in a large variety of natural and laboratory systems (e.g., supernovae, e.g., inertial confinement fusion pellet implosions). Initially, random perturbations at the interface grow exponentially in time. In the nonlinear stage of the instability, round "bubbles" of light fluid enter the heavy fluid and narrow "spikes" of heavy fluid penetrate the lighter one. Later on, the "bubbles-spikes" structure breaks down, the interface between the components becomes distorted [4–9], and the fluid volume becomes very fragmented. This is the mass mixing stage. Eventually, a transition (mixing transition) occurs to a new state where molecular mixing becomes the dominant effect [10].

The late state of the process, even before the mixing transition, represents an example of *variable density, inhomogeneous* turbulence in *incompressible* fluids. This is the subject of the present work. In particular, the purpose is to develop the kinetic theoretical approach to this class of systems.

In a pioneering work [11], Lundgren has defined a hierarchy of velocity distribution functions for inhomogeneous turbulence (but with homogeneous mass density). The one-point distribution, f_1, was defined so that $f_1(\mathbf{r}_1,\mathbf{v}_1,t)d^3\mathbf{v}_1$ is the probability that the velocity at $\mathbf{r}_1$ at time t is in the element $d^3\mathbf{v}_1$ about $\mathbf{v}_1$. The n point distributions were defined in a similar way so that $f_n(\mathbf{r}_1,\mathbf{v}_1,\ldots,\mathbf{r}_n,\mathbf{v}_n,t)d^3\mathbf{v}_1,\ldots,d^3\mathbf{v}_n$ is the joint probability that, for all $\mathbf{r}_j$, $j=1,\ldots,n$, the velocity at $\mathbf{r}_j$ at time t is in the elements $d^3\mathbf{v}_j$ about $\mathbf{v}_j$. These functions are also named velocity probability density functions (velocity PDFs). It was shown in Ref. [11] that the distributions obey a hierarchy of equations which is formally similar to the Bogolyubov-Born-Green-Kirwood-Yvon (BBGKY) hierarchy of statistical mechanics of Coulomb plasmas [12–17] (except that the distributions, f_n, represent the probability for *fluid* velocity rather than ions and electrons velocity). Closures of the hierarchy were suggested in Refs. [18,19].

The kinetic approach, with closure at the level of the kinetic equation for the one-point distribution, was further developed and extensively investigated and applied by Pope [20]. In the kinetic equation, effects beyond the mean-field approximation were modeled by terms representing drag and diffusion in velocity space, in analogy to the Fokker-Planck form of the collision integral in the kinetic theory of particles. The modeling was in the choice of the drag and diffusion coefficients as functionals of the one-point distribution and the turbulent dissipation and in the model equation for the turbulent dissipation. It was shown that the three lowest moments of this class of kinetic models [21,22] generate many successful Reynolds stress models of fluid turbulence [23].

In the present work, Lundgren's kinetic approach is extended to variable-density systems. The extension requires the proper generalization of the definition of velocity distribution, the derivation of an expression for the spacial distribution of the force in terms of the spacial distribution of mass density and velocity, and the conversion of the Euler equation to a conservation equation in phase space. In addition, it requires the identification of a small parameter that enables the reduction, by controlled approximations, of the ensemble average of the fine grain phase space conservation equation to closed kinetic equations.

The structure of the paper is as follows. The equations which govern the time evolution of mass mixing of two incompressible immiscible fluids due to Rayleigh-Taylor instability (e.g., [2,3]) are described in Sec. II. This is our specific

example for variable-density inhomogeneous turbulence in incompressible fluids. In Sec. III, an exact expression is derived for the fine grain force in terms of density and velocity fields and the effect of density variation is analyzed. The fine grain density-velocity distributions (FGDVD) are defined in Sec. IV A and an exact, explicit equation for their time evolution is presented. The average of the FGDVD is the joint velocity-density probability density function (DVPDF) and the ensemble average of the equation is an equation for the DVPDF. These equations are presented in Sec. IV B. Due to nonlinearity of the fine grain equation, the ensemble-averaged equation includes terms which are not expressible in terms of the DVPDF alone. An approximation is needed which leads to closure of the equation. The search for the small parameter is presented in Sec. V. In Sec. V A, analysis is presented based on detailed numerical solution of the Euler equations of the time evolution of the DVPDFs. It is found that the statistics of the velocity is not Gaussian. This is an indication that, indeed, a kinetic theory is required for the description of RTI mixing. In Sec. V B, it is shown that the RTI mixing system may be considered as a weakly coupled system. The lowest order of the approximations justified by the weak coupling is presented and analyzed in Sec. VI A. In Sec. VI B, it is shown that this closure properly describes the short time evolution of the system. Discussion of the results is presented in Sec. VII.

II. GOVERNING EQUATIONS

This section is devoted to the detailed description of the theoretical framework of the present paper. For definiteness, we consider planar geometry. The system of RTI mixing is initiated with the heavy, incompressible fluid of density $\rho^{(1)}$ occupying the upper half space, $z>0$, and the lighter, incompressible, fluid of density $\rho^{(2)}<\rho^{(1)}$ occupying the lowest half.

At hydrostatic equilibrium, the pressure gradient balances gravitation, i.e., $-\frac{1}{\rho}\frac{\partial}{\partial z}p=g$. This state is unstable, random perturbations at the interface will grow, and eventually will induce a mixing of the two fluids.

We follow a standard approach to RTI mixing in which the pressure $p(\mathbf{r},t)$, velocity $\mathbf{u}(\mathbf{r},t)$, and density $\rho(\mathbf{r},t)$ are assumed to be periodic in the x,y coordinates and the system is contained between two planes at $z=\pm H$, where the pressure gradient balances gravitation $[\frac{\partial}{\partial \mathbf{r}}p]_{z=H}=-\rho^{(1)}g\hat{z}$ and $[\frac{\partial}{\partial \mathbf{r}}p]_{z=-H}=-\rho^{(2)}g\hat{z}$.

In the treatment, we shall use a component indicator function $X^{(s)}(\mathbf{r},t)$ which is 1 within the volume occupied by the s component ($s=1$ for the heavy fluid and 2 for the light) and 0 elsewhere. In terms of this function, the mass density is written as

$$\rho(\mathbf{r},t)=X^{(1)}(\mathbf{r},t)\rho^{(1)}+X^{(2)}(\mathbf{r},t)\rho^{(2)} \tag{1}$$

and the mass conservation equation reduces to the a pair of equations (for $s=1,2$) [24]

$$\left(\frac{\partial}{\partial t}+\mathbf{u}\cdot\frac{\partial}{\partial \mathbf{r}}\right)X^{(s)}=0. \tag{2}$$

The Euler equation is

$$\rho\left(\frac{\partial}{\partial t}\mathbf{u}+\mathbf{u}\cdot\frac{\partial}{\partial \mathbf{r}}\mathbf{u}\right)=\mathbf{F}, \tag{3}$$

where

$$\mathbf{F}\equiv-\frac{\partial}{\partial \mathbf{r}}p-\rho g\hat{z}+\eta \tag{4}$$

and η is the force due to interfacial interaction. In treating the late stage of the RTI problem, it is not necessary to include a molecular viscosity term in the equation, since much stronger dissipation mechanisms occur in the averaged equations. [For the possible inclusion of molecular viscosity in the momentum equation and molecular diffusivity, between miscible fluids, in the mass conservation equation (2), see Appendix A].

Incompressibility imposes a relation between the force and both the velocity and density fields. To find this relation, it is necessary to solve the differential equation

$$\frac{\partial}{\partial \mathbf{r}}\cdot\left(\frac{\mathbf{F}}{\rho}\right)=\frac{1}{\rho(\mathbf{r})}S^{u}(\mathbf{r}), \tag{5}$$

with the boundary conditions at $z\to\pm\infty$, together with the requirement that p and η are periodical in the x,y plane. S^{u} in the source term of Eq. (5) is

$$S^{u}(\mathbf{r})\equiv\rho(\mathbf{r})\frac{\partial}{\partial \mathbf{r}}\cdot\left(\mathbf{u}\cdot\frac{\partial}{\partial \mathbf{r}}\mathbf{u}\right)=\rho\left[\left(\frac{\partial}{\partial \mathbf{r}}\mathbf{u}\right):\left(\frac{\partial}{\partial \mathbf{r}}\mathbf{u}\right)\right]. \tag{6}$$

The expression $(\frac{\partial}{\partial \mathbf{r}}\mathbf{u}):(\frac{\partial}{\partial \mathbf{r}}\mathbf{u})\equiv(\frac{\partial}{\partial_i}u_j)(\frac{\partial}{\partial j}u_i)$ (summation convention) in the second equality of Eq. (6) results from the first equality with the help of the incompressibility condition $\frac{\partial}{\partial_i}(u_j\frac{\partial}{\partial j}u_i)=(\frac{\partial}{\partial_i}u_j)\frac{\partial}{\partial j}u_i+\rho u_j\frac{\partial}{\partial_j}\frac{\partial}{\partial_i}u_i=(\frac{\partial}{\partial_i}u_j)(\frac{\partial}{\partial j}u_i)$.

The solution of Eq. (5) for the force $\mathbf{F}(\mathbf{r},t)$ in terms of velocity $\mathbf{u}(\mathbf{r},t)$ and density $\rho(\mathbf{r},t)$ enables the elimination of $\mathbf{F}$ from the Euler equation (3) which yields an explicit closed equation for the time evolution of the fine grain fluid variables $\mathbf{u}$ and ρ. In turn, this equation may be converted to an equation for the probability density function of $\mathbf{u}$ and ρ, which is analogous to the Klimontovich equation in nonequilibrium statistical mechanics of gases and plasmas [13,15–17] and can serve as a starting point for the derivation of kinetic equations for RTI mixing and in general for turbulence in variable-density incompressible, statistically inhomogeneous fluids. The next two sections are devoted to the derivation of the equations for the time evolution of the fine grain fluid variables and their probability density functions.

III. FINE GRAIN FORCE

In this section, an expression for the force $\mathbf{F}(\mathbf{r},t)$ in terms of velocity $\mathbf{u}(\mathbf{r},t)$ and density $\rho(\mathbf{r},t)$ is derived by solving Eq. (5). The effect of density fluctuations on the acceleration is analyzed.

It is more convenient to solve the integral form of the equation. Explicitly, the equation

$$\mathbf{F} = -\frac{1}{4\pi}\int d^3\mathbf{r}'\left\{\left(\frac{\partial}{\partial\mathbf{r}}\frac{1}{|\mathbf{r}-\mathbf{r}'|}\right)\left[\rho(\mathbf{r}')\left(\frac{\partial}{\partial\mathbf{r}'}\mathbf{u}\right):\left(\frac{\partial}{\partial\mathbf{r}'}\mathbf{u}\right)\right.\right.$$
$$\left.\left.+\frac{1}{\rho(\mathbf{r}')}\left(\frac{\partial}{\partial\mathbf{r}'}\rho(\mathbf{r}')\right)\cdot(\mathbf{F}+\rho g\hat{z})\right]\right\}$$
$$-\left(\rho-\frac{1}{2}(\rho^{(1)}+\rho^{(2)})\right)g\hat{z} \tag{7}$$

is equivalent to Eq. (5) together with the boundary conditions. Indeed, taking the divergence of Eq. (7), using the property $\frac{\partial}{\partial\mathbf{r}}\cdot\frac{\partial}{\partial\mathbf{r}}\frac{1}{|\mathbf{r}-\mathbf{r}'|}=-4\pi\delta^3(\mathbf{r}-\mathbf{r}')$ [25], we get back Eq. (5). To check that the boundary conditions are obeyed, notice that the integral in Eq. (7) has the asymptotic $\mp\frac{1}{2}g\hat{z}[\rho^{(1)}-\rho^{(2)}]$ as $z\to\mp H$.

The solution of Eq. (7) is obtained by moving the term which involves $\mathbf{F}$ to the left-hand side and inverting the operator $\{\delta^3(\mathbf{r}-\mathbf{r}')I+\frac{1}{4\pi}\int(\frac{\partial}{\partial\mathbf{r}}\frac{1}{|\mathbf{r}-\mathbf{r}'|})\frac{1}{\rho(\mathbf{r}')}[\frac{\partial}{\partial\mathbf{r}'}\rho(\mathbf{r}')]\}$. The result is

$$\mathbf{F} = \mathbf{F}^b + \mathbf{F}^{g\rho} + \mathbf{F}^{u\rho}. \tag{8}$$

The three forces in this formula are

$$\mathbf{F}^b \equiv -\left(\rho-\frac{1}{2}(\rho^{(1)}+\rho^{(2)})\right)g\hat{z}, \tag{9}$$

$$\mathbf{F}^{g\rho} \equiv -\frac{\partial}{\partial\mathbf{r}}\int G(\mathbf{r},\mathbf{r}')S^{g\rho}(\mathbf{r}')d^3\mathbf{r}', \tag{10}$$

$$\mathbf{F}^{u\rho} \equiv -\frac{\partial}{\partial\mathbf{r}}\int G(\mathbf{r},\mathbf{r}')S^{u}(\mathbf{r}')d^3\mathbf{r}', \tag{11}$$

with

$$S^{g\rho}(\mathbf{r}') \equiv \frac{1}{2}(\rho^{(1)}+\rho^{(2)})g\hat{z}\cdot\frac{1}{\rho(\mathbf{r}')}\frac{\partial}{\partial\mathbf{r}'}\rho. \tag{12}$$

The Kernel in the integrals is,

$$G(\mathbf{r},\mathbf{r}') = \int G_0(\mathbf{r}-\mathbf{r}'')\left\{\delta^3(\mathbf{r}''-\mathbf{r}')-Q(\mathbf{r}'',\mathbf{r}')\right.$$
$$\left.+\int Q(\mathbf{r}'',\mathbf{r}''')Q(\mathbf{r}''',\mathbf{r}')d^3\mathbf{r}'''-\cdots+\cdots\right\}d^3\mathbf{r}''$$
$$=\int G_0(\mathbf{r}-\mathbf{r}'')[\delta^3(\mathbf{r}''-\mathbf{r}')+Q(\mathbf{r}'',\mathbf{r}')]^{-1}d^3\mathbf{r}'' \tag{13}$$

where

$$Q(\mathbf{r},\mathbf{r}') \equiv \frac{1}{\rho(\mathbf{r})}\left(\frac{\partial}{\partial\mathbf{r}}\rho(\mathbf{r})\right)\cdot\frac{\partial}{\partial\mathbf{r}}G_0(\mathbf{r},\mathbf{r}') \tag{14}$$

and

$$G_0(\mathbf{r}-\mathbf{r}'') \equiv \frac{1}{4\pi}\frac{1}{|\mathbf{r}-\mathbf{r}''|}. \tag{15}$$

To check the solution, note that $G(\mathbf{r},\mathbf{r}')$ is the Green's function of the operator $-\rho\frac{\partial}{\partial\mathbf{r}}\cdot\frac{1}{\rho}\frac{\partial}{\partial\mathbf{r}}$, indeed

$$\rho(\mathbf{r})\frac{\partial}{\partial\mathbf{r}}\cdot\frac{1}{\rho(\mathbf{r})}\frac{\partial}{\partial\mathbf{r}}G(\mathbf{r},\mathbf{r}') = \int\left[\frac{\partial}{\partial\mathbf{r}}\cdot\frac{\partial}{\partial\mathbf{r}}-\frac{1}{\rho}\left(\frac{\partial}{\partial\mathbf{r}}\rho\right)\cdot\frac{\partial}{\partial\mathbf{r}}\right]\frac{1}{4\pi}\frac{1}{|\mathbf{r}-\mathbf{r}''|}\left[\delta^3(\mathbf{r}''-\mathbf{r}')-Q(\mathbf{r}'',\mathbf{r}')\right.$$
$$\left.+\int Q(\mathbf{r}'',\mathbf{r}''')Q(\mathbf{r}''',\mathbf{r}')d^3\mathbf{r}'''-\cdots+\cdots\right]d^3\mathbf{r}''$$
$$=\int[-\delta^3(\mathbf{r}-\mathbf{r}'')-Q(\mathbf{r},\mathbf{r}'')]\left[\delta^3(\mathbf{r}''-\mathbf{r}')-Q(\mathbf{r}'',\mathbf{r}')+\int Q(\mathbf{r}'',\mathbf{r}''')Q(\mathbf{r}''',\mathbf{r}')d^3\mathbf{r}'''-\cdots+\cdots\right]d^3\mathbf{r}''$$
$$=\left\{\left[-\delta^3(\mathbf{r}-\mathbf{r}')+Q(\mathbf{r},\mathbf{r}')-\int Q(\mathbf{r},\mathbf{r}''')Q(\mathbf{r}''',\mathbf{r}')d^3\mathbf{r}'''+\cdots\right]\right.$$
$$\left.+\left[-Q(\mathbf{r},\mathbf{r}'')+\int Q(\mathbf{r},\mathbf{r}'')Q(\mathbf{r}'',\mathbf{r}')d^3\mathbf{r}''-\cdots\right]\right\}=-\delta^3(\mathbf{r}-\mathbf{r}'). \tag{16}$$

With this result, it is readily seen that operating with $\frac{\partial}{\partial\mathbf{r}}\cdot\frac{1}{\rho}$ on $\mathbf{F}$ of Eq. (8), one gets the right-hand side of Eq. (5). The solution may be further simplified. Using the methods of Ref. [24], it may be shown that integrals involving gradients of functions of the mass density may be simplified in the form

$$\int\frac{\partial}{\partial\mathbf{r}'}\xi[\rho(\mathbf{r}',t)]\cdot\vec{f}(\mathbf{r}',t)d^3\mathbf{r}' = \left[\frac{\xi(\rho^{(1)})-\xi(\rho^{(2)})}{(\rho^{(1)}-\rho^{(2)})}\right]\int\frac{\partial}{\partial\mathbf{r}'}\rho(\mathbf{r}',t)\cdot\vec{f}(\mathbf{r}',t)d^3\mathbf{r}'. \tag{17}$$

As a result, in the expression for $\mathbf{F}$, we may replace Q by the function $\tilde{Q}$ defined as

$$\tilde{Q}(\mathbf{r}',\mathbf{r}) \equiv \left(\frac{\ln\left(\frac{\rho^{(1)}}{\rho^{(2)}}\right)}{(\rho^{(1)}-\rho^{(2)})} \right) \left(\frac{\partial}{\partial \mathbf{r}'} \rho(\mathbf{r}') \right) \cdot \frac{\partial}{\partial \mathbf{r}} G_0(\mathbf{r}',\mathbf{r}). \tag{18}$$

In the limit of homogeneous density $\rho(\mathbf{r})=\rho^{(1)}=\rho^{(2)}=\rho_0$, the solution (8) reduces to the well-known result [26]

$$\mathbf{F}_0 = \int \frac{\partial}{\partial \mathbf{r}} G_0(\mathbf{r},\mathbf{r}') S_0^u(\mathbf{r}') d^3\mathbf{r}', \tag{19}$$

where

$$S_0^u(\mathbf{r}') = \rho_0 \left(\frac{\partial}{\partial \mathbf{r}'} \mathbf{u} \right) : \left(\frac{\partial}{\partial \mathbf{r}'} \mathbf{u} \right).$$

Relation (19) is a bi-linear relation between the force and the velocity field. As is clear from the form of the Green's function [Eq. (13)], density variation introduces a strong nonlinear dependence of the force on the density gradient.

We proceed in analyzing the physical origin of the various terms in relation (8). To this end, we rewrite the Green's function (13) as

$$\frac{\partial}{\partial \mathbf{r}} G(\mathbf{r},\mathbf{r}_N) = \sum_{n=0}^{\infty} \mathbf{T}_n(\mathbf{r},\mathbf{r}_N), \tag{20}$$

where the terms $\mathbf{T}_n$ are defined by the differential recursive relation

$$\mathbf{T}_0 \equiv \frac{\partial}{\partial \mathbf{r}} G_0(\mathbf{r},\mathbf{r}_N), \tag{21}$$

$$\frac{\partial}{\partial \mathbf{r}} \cdot \mathbf{T}_n(\mathbf{r},\mathbf{r}_N) = -S_n(\mathbf{r},\mathbf{r}_N), \tag{22}$$

$$S_n(\mathbf{r},\mathbf{r}_N) = \frac{1}{\rho(\mathbf{r})} \left(\frac{\partial}{\partial \mathbf{r}} \rho(\mathbf{r}) \right) \cdot \mathbf{T}_{n-1}(\mathbf{r},\mathbf{r}_N). \tag{23}$$

The first term in the sum (20) is the "direct" pressure gradient described by the "bare" Green's function for the case of a point source in uniform mass density $\mathbf{T}_0(\mathbf{r},\mathbf{r}_N)=\frac{\partial}{\partial \mathbf{r}} G_0(\mathbf{r},\mathbf{r}_N) = \frac{\partial}{\partial \mathbf{r}} \left(\frac{1}{4\pi} \frac{1}{|\mathbf{r}-\mathbf{r}_N|} \right)$ [i.e., the solution of $\frac{\partial}{\partial \mathbf{r}} \cdot \mathbf{T}_0(\mathbf{r},r_N) = \delta^3(\mathbf{r}-\mathbf{r}_N)$]. The second contribution, T_1, is the correction due to secondary source, generated by the interaction of the direct pressure with a density fluctuation [i.e., the solution of $\frac{\partial}{\partial \mathbf{r}} \cdot \mathbf{T}_1(\mathbf{r},\mathbf{r}_N) = S_1 = \frac{1}{\rho(\mathbf{r})} \frac{\partial}{\partial \mathbf{r}} \rho(\mathbf{r}) \cdot \mathbf{T}_0(\mathbf{r},\mathbf{r}_N)$]. In general, the n order correction is due to the source generated by the interaction of the $n-1$ order pressure with the density fluctuations. Equation (20) represents the sum of the bare field and fields due to the virtual sources, S_n.

The various terms in relation (8) may be described as follows: $\mathbf{F}^b$ is the buoyancy force. $\mathbf{F}^{g\rho}$ represents the force due to the "secondary source" $S^{g\rho}$ generated by the interaction of the gravitational force with density variation. $\mathbf{F}^{u\rho}$ represents the force due to the source S^u. This is the only term which survives in the absence of density variation and gravity. The effect of density variation on $\mathbf{F}^{u\rho}$ is in the "dressing" of the bare Green's function G_0 by the function $[I+Q]^{-1}$ which represents the sum of the contributions of secondary and higher-order sources due to density fluctuations.

Another consequence of relation (8) is that gravitation and density variation do not alter the average acceleration. To see this result, note that the acceleration $\mathbf{a}=\frac{1}{\rho}\mathbf{F}$ may be decomposed in the form

$$\mathbf{a} = \mathbf{a}_0 + \Delta\mathbf{a}, \tag{24}$$

where the correction term is

$$\Delta\mathbf{a} \equiv \frac{1}{\rho}\mathbf{F}^b + \frac{1}{\rho}\mathbf{F}^{g\rho} - \left\{ \frac{1}{\rho(\mathbf{r})} \frac{\partial}{\partial \mathbf{r}} G(\mathbf{r},\mathbf{r}')\rho(\mathbf{r}') - \frac{\partial}{\partial \mathbf{r}} G_0(\mathbf{r},\mathbf{r}') \right\} \frac{1}{\rho(\mathbf{r}')} S^u(\mathbf{r}') d^3\mathbf{r}'. \tag{25}$$

The correction $\Delta\mathbf{a}$ vanishes at $z \to \pm\infty$; also by Eqs. (15) and (16) we get

$$\frac{\partial}{\partial \mathbf{r}} \cdot \Delta\mathbf{a} = 0. \tag{26}$$

By Eq. (26) together with Gauss theorem, we see that the average of the correction term vanishes

$$\langle \Delta\mathbf{a} \rangle = 0 \tag{27}$$

and

$$\langle \mathbf{a} \rangle = \langle \mathbf{a}_0 \rangle, \tag{28}$$

i.e., the average acceleration is not affected neither by gravity nor by density fluctuations. Still, correlations in the system (e.g., $\langle \mathbf{ua} \rangle$) are affected by density fluctuations.

In Eqs. (27) and (28), the angular brackets $\langle \cdots \rangle$ denote ensemble average. Our system is statistically one-dimensional [20], i.e., it is statistically invariant to translation in the (x,y) plane and to rotation around the z axis. In such systems, the ensemble average is equivalent to the average over the (x,y) plane in a single realization, i.e.,

$$\langle \cdots \rangle = \frac{1}{L^2} \int_{-L}^{L} dx \int_{-L}^{L} dy \{ \cdots \}, \tag{29}$$

where L is the transverse periodicity length. (In the simulation which is only in two dimensions, $\frac{1}{L^2}\int_{-L}^{L}dx\int_{-L}^{L}dy$ is replaced by $\frac{1}{L}\int_{-L}^{L}dy$.)

Equation (24) may be further interpreted in analogy with the electric field in macroscopic media (see, for example, Sec. I.4 in [25]) where $\mathbf{a}_0$ is analogous to the electric field, $\mathbf{a}$ is analogous to the electric displacement, and $\Delta\mathbf{a}$ is analogous to the contribution of the sources within the medium. Like the electric field and electric displacement, both $\mathbf{a}$ and $\mathbf{a}_0$ obey the same equation $\frac{\partial}{\partial \mathbf{r}} \cdot \mathbf{a} = \frac{\partial}{\partial \mathbf{r}} \cdot \mathbf{a}_0 = \frac{1}{\rho} S^u$.

IV. EQUATIONS FOR THE FINE GRAIN DISTRIBUTION AND THE DENSITY-VELOCITY PROBABILITY DENSITY FUNCTION

A. Equations for the fine grain distribution

The detailed information about the flow in incompressible RTI system is in the velocity and mass density fields $\mathbf{u}(\mathbf{r},t),\rho(\mathbf{r},t)$. This information may also be incorporated into a pair of the FGDVD defined by

$$F_1^{(s)}(\mathbf{r},\mathbf{v},t) \equiv X^{(s)}(\mathbf{r},t)\delta^3[\mathbf{u}(\mathbf{r},t)-\mathbf{v}]. \tag{30}$$

Indeed, these functions generate the fields through the relations

$$\mathbf{u} = \sum_{s=1}^{2} \int \mathbf{v} F_1^{(s)} d^3\mathbf{v}, \tag{31}$$

$$X^{(s)} = \int F_1^{(s)} d^3\mathbf{v}, \tag{32}$$

$$\rho = \sum_{s=1}^{2} \rho^{(s)} \int F_1^{(s)} d^3\mathbf{v}, \tag{33}$$

and also

$$\frac{1}{\rho} = \sum_{s=1}^{2} \frac{1}{\rho^{(s)}} \int F_1^{(s)} d^3\mathbf{v}. \tag{34}$$

The right-hand side in the incompressibility equation (5) and the function $\tilde{Q}$ may also be expressed in terms of the FGDVDs as

$$\frac{1}{\rho(\mathbf{r})} S^u(\mathbf{r}) = \sum_{s=1}^{2} \int \left(\mathbf{v}\cdot\frac{\partial}{\partial \mathbf{r}}\right)^2 F_1^{(s)} d^3\mathbf{v} \tag{35}$$

and

$$\tilde{Q}(\mathbf{r}',\mathbf{r}) \equiv \left(\frac{\ln\left(\frac{\rho^{(1)}}{\rho^{(2)}}\right)}{(\rho^{(1)}-\rho^{(2)})}\right) \times \left(\frac{\partial}{\partial \mathbf{r}'} \sum_{s'=1}^{2} \rho^{(s')} \int F_1^{(s')} d^3\mathbf{v}'\right) \cdot \frac{\partial}{\partial \mathbf{r}} G_0(\mathbf{r}',\mathbf{r}).$$

With these relations, Eqs. (8), (24), and (25) for the force and the acceleration may be expressed in terms of $\rho^{(1)}$, $\rho^{(2)}$, and the FGDVD.

In order to simplify the evaluation of products of fluid variables at different positions, we define the multipoint FGDVDs as

$$F_n^{(s_1,\ldots,s_n)}(\mathbf{r}_1,\mathbf{v}_1,\ldots,\mathbf{r}_n,\mathbf{v}_n,t) \equiv F_1^{(s_1)}(\mathbf{r}_1,\mathbf{v}_1,t)\cdots F_1^{(s_n)}(\mathbf{r}_n,\mathbf{v}_n,t). \tag{36}$$

To derive the equations for the time evolution of the fine grain distribution, $F_1^{(s)}$, as defined in Eq. (30), one starts by using the Euler Eq. (3) by which the time derivative of the delta function is

$$\frac{\partial}{\partial t}[\delta^3(\mathbf{u}-\mathbf{v})] = \frac{\partial}{\partial t}\mathbf{u}\cdot\frac{\partial}{\partial \mathbf{u}}\delta^3(\mathbf{u}-\mathbf{v}) = \left(-\mathbf{u}\cdot\frac{\partial}{\partial \mathbf{r}}\mathbf{u}+\mathbf{a}\right)\cdot\frac{\partial}{\partial \mathbf{u}}\delta^3(\mathbf{u}-\mathbf{v}). \tag{37}$$

Using the chain rule for derivatives $\mathbf{u}\cdot\frac{\partial}{\partial \mathbf{r}}\mathbf{u}\frac{\partial}{\partial \mathbf{u}}\delta^3(\mathbf{u}-\mathbf{v}) = \mathbf{u}\cdot\frac{\partial}{\partial \mathbf{r}}\delta^3(\mathbf{u}-\mathbf{v})$, in Eq. (37) multiplying it by $X^{(s)}$, one gets

$$X^{(s)}\left(\frac{\partial}{\partial t}+\mathbf{u}\cdot\frac{\partial}{\partial \mathbf{r}}\right)\delta^3(\mathbf{u}-\mathbf{v}) = \mathbf{a}\cdot\frac{\partial}{\partial \mathbf{u}}[X^{(s)}\delta^3(\mathbf{u}-\mathbf{v})]. \tag{38}$$

Next we multiply Eq. (2) by $[\delta^3(\mathbf{u}-\mathbf{v})]$ and add the result to Eq. (38). This process yields the equation for the FGDVD

$$\frac{d}{dt}F_1^{(s)}(\mathbf{r},\mathbf{v},t) = \left[\frac{\partial}{\partial t}+\mathbf{v}\cdot\frac{\partial}{\partial \mathbf{r}}+\mathbf{a}(\mathbf{r},t)\cdot\frac{\partial}{\partial \mathbf{v}}\right]F_1^{(s)}(\mathbf{r},\mathbf{v},t) = 0. \tag{39}$$

For the manipulations below, we need a more efficient indexing of the variables. We use the shorthand X_j for phase space variables (including the component index s), i.e.,

$$X_j = s_j,\mathbf{r}_j,\mathbf{v}_j. \tag{40}$$

For example, the fine grain function $F_1^{(s_j)}(\mathbf{r}_j,\mathbf{v}_j,t)$ will be denoted by $F(j)$ and integration over phase space is denoted by

$$\int dX_j \equiv \sum_{s_j=1}^{2} \int d^3\mathbf{v}_j d^3\mathbf{r}_j. \tag{41}$$

With this notation, Eq. (39) reads

$$\frac{d}{dt}F_1(1) = \left[\frac{\partial}{\partial t}+\mathbf{v}_1\cdot\frac{\partial}{\partial \mathbf{r}}+\mathbf{a}(\mathbf{r}_1,t)\cdot\frac{\partial}{\partial \mathbf{v}_1}\right]F_1(1) = 0. \tag{42}$$

Equation (42) immediately yields also an equation for F_n,

$$\frac{d}{dt}F_n(1,\ldots,n) = \left[\frac{\partial}{\partial t}+\sum_{j=1}^{n}\left(\mathbf{v}_j\cdot\frac{\partial}{\partial \mathbf{r}_j}+\mathbf{a}(\mathbf{r}_j,t)\cdot\frac{\partial}{\partial \mathbf{v}_j}\right)\right]F_n(1,\ldots,n) = 0. \tag{43}$$

Equation (42) is analogous to the Klimontovich equation in nonequilibrium statistical mechanics of gases and plasmas [13,15–17]. Together with the expression for $\mathbf{a}$, it constitutes an exact, explicit, and closed pair of equations for $F_1^{(s)}$ $(s=1,2)$. No statistical averaging is involved.

B. Equation for the density-velocity probability density function

The ensemble average of Eq. (42) is

$$\left[\frac{\partial}{\partial t}+\mathbf{v}\cdot\frac{\partial}{\partial \mathbf{r}}\right]\langle F_1(1)\rangle = -\frac{\partial}{\partial \mathbf{v}}\cdot\langle \mathbf{a}(\mathbf{r},t)F_1(1)\rangle. \tag{44}$$

The last equation is an unclosed equation for, $f_1(1)$ defined by

$$f_1(1) \equiv \langle F_1(1)\rangle = \langle X^{(s_1)}(\mathbf{r}_1,t)\delta^3[\mathbf{u}(\mathbf{r}_1,t)-\mathbf{v}_1]\rangle, \quad (45)$$

which is the probability of having a point within the component (s_1) with velocity $\mathbf{v}_1$ at position $\mathbf{r}_1$. In practice, it may be obtained from the experimental measurements of the velocity and mass density fields (e.g., [27]) or from solutions of the time evolution of the ensemble of systems by counting all the realizations in which the point $\mathbf{r}_1$ is within the component s_1 and the velocity $\mathbf{u}(\mathbf{r}_1,t)$ equals $\mathbf{v}_1$ and then dividing by the total number of realizations. We shall call this function the one-point DVPDF. The normalization of f_1 is such that

$$\int f_1 dX_1 = \int \left\langle \sum_{s=1}^{2} X^{(s)}(\mathbf{r},t) \right\rangle d^3\mathbf{r} = V,$$

where V is the volume which is occupied by system.

With definition (45), the combination $\rho^{(1)}f_1^{(1)}(\mathbf{r}_1,\mathbf{v}_1,t)+\rho^{(2)}f_1^{(2)}(\mathbf{r}_1,\mathbf{v}_1,t)=\langle\rho(\mathbf{r}_1,t)\delta^3[\mathbf{u}(\mathbf{r}_1,t)-\mathbf{v}_1]\rangle$ coincides with the probability density function suggested by Polyakov [28] for the description of turbulence. For the case of constant density, this definition coincides with the velocity distribution, $\langle\delta^3[\mathbf{u}(\mathbf{r}_1,t)-\mathbf{v}_1]\rangle$, suggested by Lundgren [11].

Using the decomposition (24) and the explicit form of $\mathbf{a}_0$ in terms of F_1, we rewrite Eq. (44) in the form

$$\left[\frac{\partial}{\partial t}+\mathbf{v}_1\cdot\frac{\partial}{\partial \mathbf{r}_1}\right]f_1(1) = -\int dX_2 V_0(1,2)f_2(1,2) - \frac{\partial}{\partial \mathbf{v}_1}\cdot\langle\Delta\mathbf{a}(\mathbf{r}_1,t)F_1(1)\rangle, \quad (46)$$

where the operator V_0 is defined by

$$V_0(i,j) \equiv \Omega^2(j)\left(\frac{\partial}{\partial \mathbf{r}_i}G_0(\mathbf{r}_i,\mathbf{r}_j)\right)\cdot\frac{\partial}{\partial \mathbf{v}_i},$$

$$\Omega(j) \equiv \mathbf{v}_j\cdot\frac{\partial}{\partial \mathbf{r}_j}. \quad (47)$$

The two-point DVPDF is

$$f_2(1,2) \equiv \langle F_2(1,2)\rangle$$

and in general

$$f_n(1,\ldots,n) \equiv \langle F_n(1,\ldots,n)\rangle.$$

The set of coupled equations for $f_1, f_2, \ldots$, obtained from Eq. (43), is

$$\left[\frac{\partial}{\partial t}+\sum_{j=1}^{n}\mathbf{v}_j\cdot\frac{\partial}{\partial \mathbf{r}_j}\right]f_n(1,\ldots,n) = -\sum_{j=1}^{n}\int dX_{n+1}V_0(j,n+1)f_{n+1}(1,\ldots,n+1) - \sum_{j=1}^{n}\frac{\partial}{\partial \mathbf{v}_j}\cdot\langle\Delta\mathbf{a}(\mathbf{r}_j,t)F_n(1,\ldots,n)\rangle. \quad (48)$$

In the set of Eqs. (48), only the last term on the right-hand side represents the effect of gravity and density variation. Without this term, we are left with the hierarchy of equations derived by Landgren [11] for turbulence with constant density.

These equations are also formally similar to the equations which are used as a starting point for the kinetic theory of plasmas (see, for example, Appendix A in Ref. [17]). The difference is in the interaction operator V_0 which in the plasma case takes the form

$$V_{0\,\mathrm{Plasma}}(i,j) = \omega_p^2\frac{\partial}{\partial \mathbf{r}_i}G_0(\mathbf{r}_i-\mathbf{r}_j)\cdot\frac{\partial}{\partial \mathbf{v}_i}, \quad (49)$$

where ω_p is the plasma frequency

$$\omega_p \equiv \sqrt[2]{\frac{4\pi n_0 e^2}{m^{(s_j)}}}$$

(e is the electron charge and $m^{(s_i)}$ is the electron or ion mass: $s_1=1$ for electron and $s_i=2$ for ions).

The dependence of the interaction operator on the characteristic time in the plasma ω_p^{-1} enables a systematic analysis of the relative size of the different terms in the equations. This analysis justifies approximations which lead to closure of the kinetic equations (e.g., Bogolubov's hierarchy of time scales [12]). In the fluid turbulence case, the interaction operator V_0 and in particular Ω does not depend on physical constants. Therefore, we could not adapt the systematic treatment of plasma kinetic theory to our case. Instead, we have examined the relative size of terms in the kinetic equations by using the DVPDF compiled from numerical solutions of the Euler equations. This analysis is described in the next section.

V. PROPERTIES OF THE KINETIC EQUATIONS AND THE VPDF

In the following two sections, we shall analyze results compiled from two-dimensional solutions of the Euler equation using the hydro code LEEOR2D. This code was used in the past, in numerous works, for the analysis of the RTI mixing (e.g., [29]) and for the determination of the rate of expansion of the mixing zone in the self-similar regime. In the present work, the same fine grain solutions of pressure density and velocity fields will be used for the analysis of the properties of the DVPDFs.

The simulation was initiated in a state closed to an hydrostatic equilibrium with the heavy fluid, at rest, filling the upper half of the volume $[z>\delta z(y)]$ with fluid 1 with density $\rho_0(1)=\rho^{(1)}e^{-g/C_{\mathrm{sound}}^2 z}\sim\rho^{(1)}$ and the light fluid 2, also at rest, filling the lower half with density $\rho_0(2)=\rho^{(2)}e^{-g/C_{\mathrm{sound}}^2 z}\sim\rho^{(2)}$. The deviation of the interface from $z=0$, δz, was

$$\delta z(y) = 0.01\sum_{l=160}^{l=320}\phi_l\cos\left(\frac{\pi y l}{L}\right),$$

where ϕ_l was chosen randomly for each mode as +1 or −1. Incompressibility was imposed by using an equation of state, which determined the pressure p from the density ρ separately for fluid $s=1$ or $s=2$ by $p=C_{\mathrm{sound}}^2(\rho-\rho^{(s)})$ with a very large value of sound velocity C_{sound} (see Sec. 3.6 in Ref. [35]), i.e., $\frac{g}{C_{\mathrm{sound}}^2}H\ll 1$. The gravitational acceleration in the

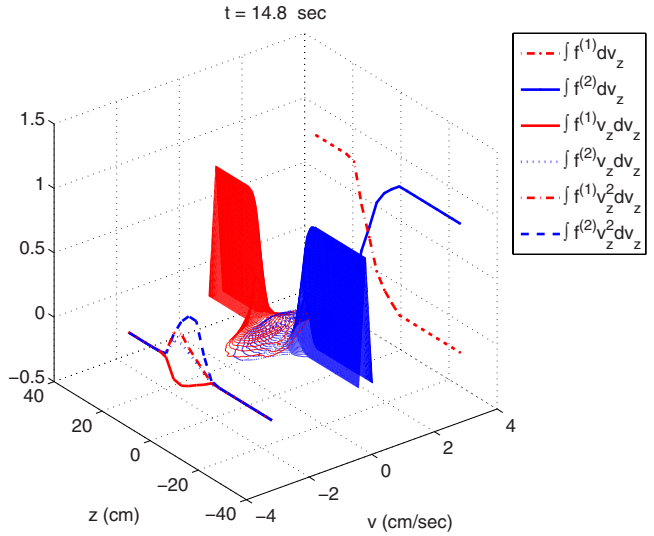

FIG. 1. (Color online) Contours of the axial DVPDFs $f^{(1)}$ and $f^{(2)}$ at $t=14.8$ s (legend corresponds to lines on walls).

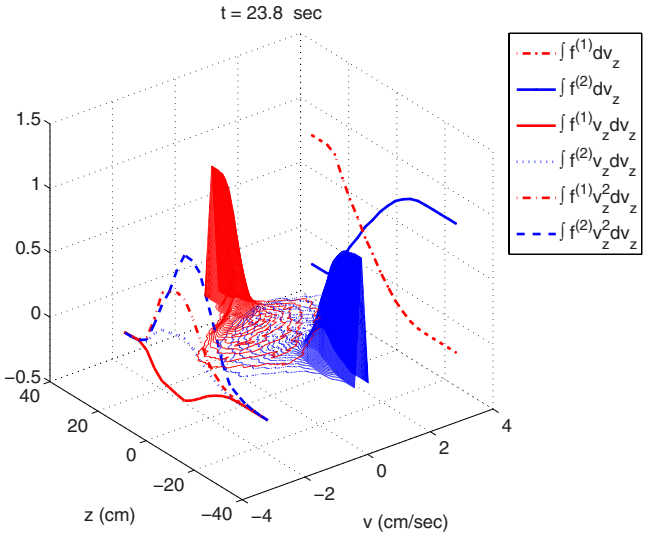

FIG. 2. (Color online) Same as Fig. 1 at $t=23.8$.

simulation was 1 cm s^{-2} and the initial Atwood number, $A \equiv \frac{\rho^{(1)}-\rho^{(2)}}{\rho^{(1)}+\rho^{(2)}}$, was 0.5 (natural densities $\rho^{(1)}=3$, $\rho^{(2)}=1$). The dimensions of the simulation region were $L=200$ cm by $2H=62.5$ cm. The grid sizes were $N_y=1280$ and $N_z=400$. Some more details of the numerical scheme and convergence tests are presented in Appendix B.

A. Density-velocity probability density functions

The one-point DVPDF in a statistically one-dimensional (1D) system has the following property:

$$f_1^{(s)}(\mathbf{r},\mathbf{v},t) = f_1^{(s)}(z,\mathbf{v},t). \tag{50}$$

We define the axial DVPDF for the axial velocity by

$$f^{(s)}(z,v_z,t) \equiv \int f_1^{(s)}(z,\mathbf{v},t)dv_y dv_x = \langle X^{(s)}\delta(u_z - v_z)\rangle. \tag{51}$$

The averaged axial quantities are obtained as moments of the distribution

$$\langle X^{(s)}u_z^n\rangle = \int_{-\infty}^{\infty} v_z^n f^{(s)}(z,v_z,t)dv_z. \tag{52}$$

Another quantity which is of interest for mixing due to RTI, h, the extension of the mixing zone, may be evaluated from the DVPDF as the range in which $[\int_{-\infty}^{\infty} f^{(1)}(z,v_z,t)dv_z][\int_{-\infty}^{\infty} f^{(2)}(z,v_z',t)dv_z']$ does not vanish.

Figures 1 and 2 show the time evolution of the axial DVPDFs $f^{(s)}$ and the three lowest moments $\langle X^{(s)}\rangle, \langle X^{(s)}u_z\rangle, \langle X^{(s)}u_z^2\rangle$, compiled from two-dimensional solutions of the Euler equation. To further characterize the axial DVPDFs, we have looked at cuts of constant z. Figures 3 and 4 show cuts of the distribution. To these lines, we have added lines of the functions

$$f_{\mathrm{LTE}}^{(s)}(z,v_z,t) \equiv \left(\frac{\rho^{(s)}\alpha^{(s)}}{-2\pi\tau^{(s)}}\right)^{1/2} e^{\rho^{(s)}\alpha^{(s)}(v_z-U^{(s)})^2/2\tau^{(s)}}\alpha^{(s)}, \tag{53}$$

which represent a state of local "thermodynamic equilibrium" around the local averaged velocity, $U^{(s)}(z,t) \equiv \frac{1}{\langle X^{(s)}\rangle}\langle X^{(s)}u_z\rangle$, with a local "temperature" $-\tau^{(s)}(z,t) \equiv -\rho^{(s)}[\langle X^{(s)}u_z^2\rangle - \langle X^{(s)}\rangle(U^{(s)})^2]$ and local mass density $\rho^{(s)}\alpha^{(s)}(z,t)$, where $\alpha^{(s)} \equiv \langle X^{(s)}\rangle$.

From these figures, it is clear that the distributions are closed but do not entirely coincide with the distributions expected at LTE. This means that a one-point fluid theory or model (i.e., equations for the three lowest moments, $\rho^{(s)}\alpha^{(s)}$, $U^{(s)}$, $\tau^{(s)}$) cannot capture all the effects involved in RTI mixing. The deviation of the DVPDFs from Gaussian empa-

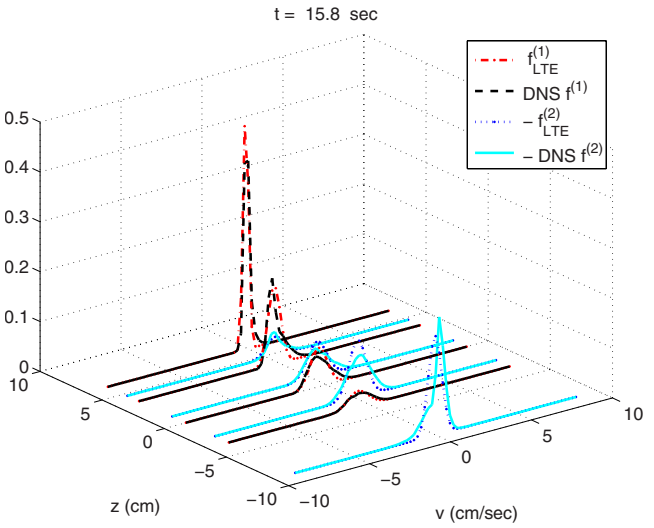

FIG. 3. (Color online) Comparison between the axial DVPDF, $f^{(s)}$ obtained directly from detailed solution of the Euler equation (simulation), and the LTE function $f_{\mathrm{LTE}}^{(s)} \equiv (\frac{\rho^{(s)}\alpha^{(s)}}{-2\pi\tau^{(s)}})^{1/2} e^{\rho^{(s)}\alpha^{(s)}(v_z-U^{(s)})^2/2\tau^{(s)}}\alpha^{(s)}$ at $t=15.8$ s.

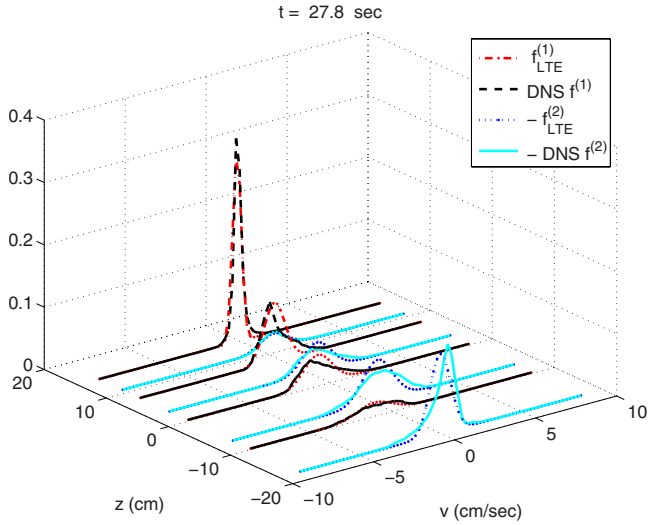

FIG. 4. (Color online) Same as Fig. 3, at $t=27.8$ s.

thizes the need for a kinetic theoretical approach of the RTI mixing process. The next section is devoted to the identification of a small parameter which enables the derivation of closed kinetic equations.

B. RTI mixing as a weakly coupled statistical system

Adding $\langle \mathbf{a} \rangle \langle F_1^{(s)} \rangle$ to both sides of Eq. (44), we get

$$\left[\frac{\partial}{\partial t} + \mathbf{v} \cdot \frac{\partial}{\partial \mathbf{r}} + \langle \mathbf{a} \rangle \cdot \frac{\partial}{\partial \mathbf{v}} \right] f^{(s)}(\mathbf{r}, \mathbf{v}, t)$$

$$= - \frac{\partial}{\partial \mathbf{v}} \cdot \langle [\mathbf{a} - \langle \mathbf{a} \rangle] X^{(s)} \delta^3(\mathbf{u} - \mathbf{v}) \rangle. \tag{54}$$

Integrating over $dv_x dv_y$ and using the property $f_1^{(s)}(\mathbf{r}, \mathbf{v}, t) = f_1^{(s)}(z, \mathbf{v}, t)$, $\langle \mathbf{a} \rangle = \hat{z} \langle a_z \rangle$, we get

$$\left[\frac{\partial}{\partial t} + v_z \frac{\partial}{\partial z} + \langle a_z \rangle \frac{\partial}{\partial v_z} \right] f^{(s)}(z, v_z, t)$$

$$= - \frac{\partial}{\partial v_z} \langle [a_z - \langle a_z \rangle] X^{(s)} \delta(u_z - v_z) \rangle. \tag{55}$$

The relative sizes of the terms in this equation are analyzed by using results compiled from the detailed solutions of the Euler equations. The DVPDFs, $f^{(s)}$, and $\langle \frac{1}{\rho} \frac{\partial}{\partial z} p X^{(s)} \delta(u_z - v_z) \rangle$ are evaluated directly from the velocity, density, and pressure fields. Terms which contain the probability density function of the interfacial interaction $\langle \frac{1}{\rho} \eta_z X^{(s)} \delta(u_z - v_z) \rangle$ are evaluated by velocity integral of Eq. (55), e.g.,

$$\left\langle \left[\frac{1}{\rho} \frac{\partial}{\partial z} p - \frac{1}{\rho} \eta_z \right] X^{(s)} \delta(u_z - v_z) \right\rangle$$

$$= \int_{-\infty}^{v} \left[\frac{\partial}{\partial t} + v_z' \frac{\partial}{\partial z} \right] f^{(s)}(z, v_z', t) dv_z' - g f^{(s)}(z, v_z, t). \tag{56}$$

Figures 5 and 6 show that for the system under consideration, the two terms in the flux on the right-hand side of Eq. (55) are very close to each other, i.e.,

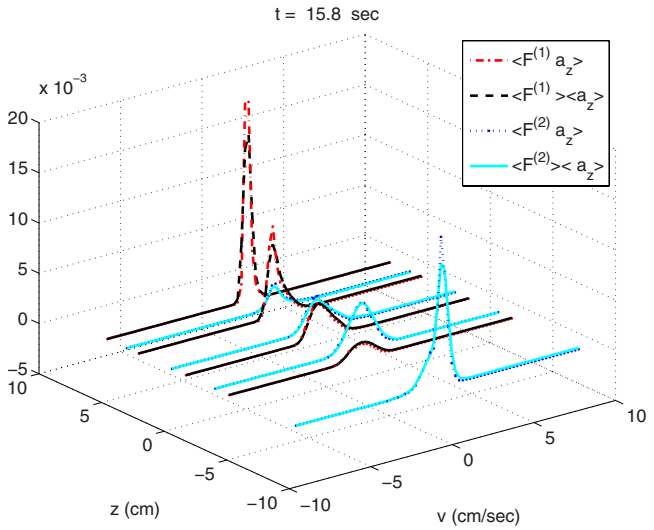

FIG. 5. (Color online) Cuts of $\langle \frac{1}{\rho} \frac{\partial}{\partial z} p + g - \frac{1}{\rho} \eta_z \rangle \langle X^{(s)} \delta(u_z - v_z) \rangle$ and $\langle (\frac{1}{\rho} \frac{\partial}{\partial z} p + g - \frac{1}{\rho} \eta_z) X^{(s)} \delta(u_z - v_z) \rangle$ at $t=15.8$ s.

$$\frac{\langle [a_z - \langle a_z \rangle] X^{(s)} \delta(u_z - v_z) \rangle}{\langle a_z \rangle \langle X^{(s)} \delta(u_z - v_z) \rangle} \ll 1. \tag{57}$$

This is an indication of the weak correlation between the acceleration and the FGDVD. This property will be utilized for approximations in the theory.

VI. CLOSURE

The next two sections will be devoted to the closure problem. In Sec. VI A, we will analyze the lowest-order approximation allowed by inequality (57) and discuss possible higher-order approximations. Section VI B will be devoted to the direct testing of the lowest-order approximation.

A. Mean-field approximation and beyond

Neglecting the right-hand side of Eq. (55), one is left with a closed equation in which the only force is the mean field

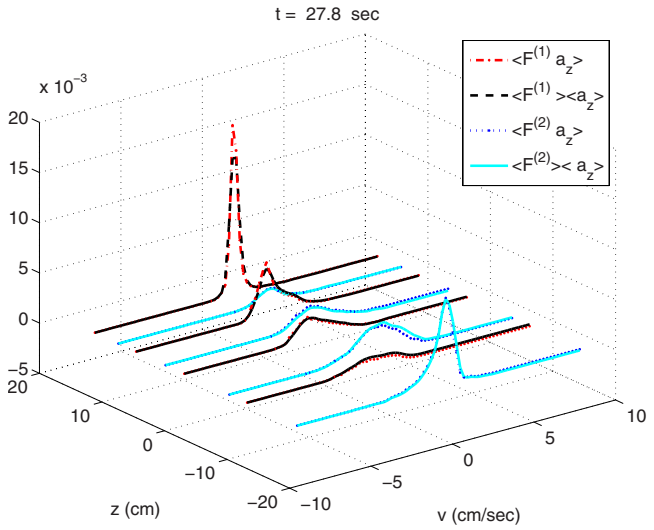

FIG. 6. (Color online) Same as Fig. 5, at $t=27.8$ s.

$\langle \mathbf{a} \rangle$. Also from the average of Eq. (3) divided by ρ, since $\frac{\partial}{\partial t}\langle \mathbf{u} \rangle = 0$, we get

$$\langle \mathbf{a} \rangle = \hat{\mathbf{z}} \left(\frac{\partial}{\partial z} \langle u_z^2 \rangle \right).$$

Therefore, the approximate closed kinetic equation is

$$\left[\frac{\partial}{\partial t} + v \frac{\partial}{\partial z} + \left(\frac{\partial}{\partial z} \sum_{s'=1}^{2} \int v_z^2 f^{(s')}(v_z', z', t) dv_z' \right) \frac{\partial}{\partial v_z} \right] f^{(s)}(z, v_z, t) \simeq 0. \quad (58)$$

This is the lowest order of the approximations justified by the inequality (57).

The right-hand side of Eq. (54) represents all the effects beyond the mean field which are neglected in Eq. (58). To make the connection to Eq. (46) and the general set of coupled Eqs. (48), we apply the cluster expansion to the multiple point functions, e.g.,

$$f_2(1,2) = f_1(1) f_1(2) + g_2(1,2),$$

$$f_3(1,2,3) = f_1(1) f_1(2) f_1(3) + f_1(1) g_2(2,3) + f_1(2) g_2(1,3) + f_1(3) g_2(1,2) + g_3(1,2,3) \quad (59)$$

(this may be viewed as the definition of the irreducible correlations g_2, g_3, etc.). With this definition, the term $\int dX_2 V_0(1,2) f_2(1,2)$ splits into the mean-field term and the correlated term and Eq. (46) takes the form

$$\left[\frac{\partial}{\partial t} + \mathbf{v}_1 \cdot \frac{\partial}{\partial \mathbf{r}_1} + \left(\frac{\partial}{\partial z} \sum_{s'=1}^{2} \int v_z^2 f^{(s')}(v_z', z', t) dv_z' \right) \hat{z} \frac{\partial}{\partial \mathbf{v}} \right] f_1(1) = - \int dX_2 V_0(1,2) g_2(1,2) - \frac{\partial}{\partial \mathbf{v}_1} \cdot \langle \Delta \mathbf{a}(\mathbf{r}_1, t) F_1(1) \rangle. \quad (60)$$

As mentioned before, due to the nonlinearity of $\Delta \mathbf{a}(\mathbf{r}_1, t)$ in ρ, the term $\frac{\partial}{\partial \mathbf{v}_1} \langle \Delta \mathbf{a}(\mathbf{r}_1, t) F_1(1) \rangle$ introduces a coupling to all multipoint functions. The weakness of coupling observed in Fig. 5 [i.e., inequality (57)] justifies the neglect of the right-hand side of Eq. (60) which includes both the effect of two point correlations in the absence of density variation $[g_2(1,2)]$ and the effect of gravity and density variation $(\Delta \mathbf{a})$. The next section will be devoted to testing the lowest-order approximation.

B. Testing the mean-field approximation

In order to test the capacity of the closed kinetic equation in the mean-field approximation (and to prepare a tool to test other possible kinetic models), we have constructed a computer program which solves kinetic equations of the form $\frac{\partial}{\partial t} f^{(s)}(z, v_z, t) = -\frac{\partial}{\partial z} \Gamma_z(f^{(s)}, v_z, z) - \frac{\partial}{\partial v_z} \Gamma_v(f^{(s)}, v_z, z)$ (in Eq. (58), $\Gamma_z = v_z f^{(s)}$ and $\Gamma_v = \{ \frac{\partial}{\partial z} \int_{-\infty}^{\infty} v_z^2 [f^{(1)}(z, v_z, t) + f^{(2)}(z, v_z, t)] dv_z \} f^{(s)}$). The program solves the kinetic equations by flux corrected transport algorithm [30,31].

In the test of Eq. (58), the DVPDFs $f^{(1)}(z, v_z, t), f^{(2)}(z, v_z, t)$ at $t = 20$ s compiled from the detailed numerical solution of the Euler equation were used as initial conditions, which were than propagated, by solving Eq. (58) for 1 s (in 25 substeps) to generate the DVPDFs at $t = 21$.

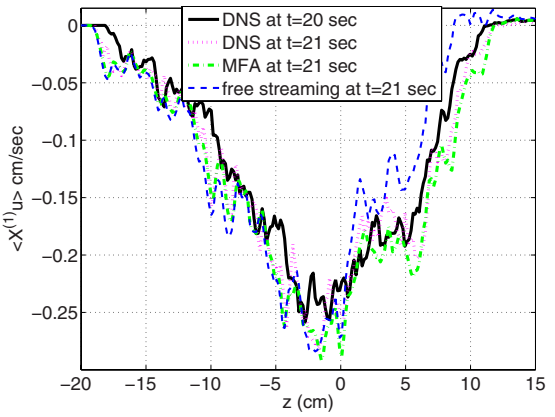

FIG. 7. (Color online) Test of the mean-field approximation.

In Figs. 7 and 8, the black solid line denote z profiles of the first moment of the DVPDF $\langle X^{(s)} u_z \rangle = \int v_z f^{(s)} dv_z$ at time $t = 20$ s, compiled from detailed numerical solutions of the Euler equation. The green dotted-dashed lines denote the first moment of the DVPDF at time $t = 21$ s obtained by the solution of the kinetic equation (58). The magenta dotted lines denote the first moment of the DVPDF at $t = 21$ compiled from the detailed numerical solutions of the Euler equation. The blue dashed lines denote the first moment of the DVPDF at time $t = 21$ s obtained by the solution of the kinetic free streaming equation $[\frac{\partial}{\partial t} + v \frac{\partial}{\partial z}] f^{(s)}(z, v_z, t) \simeq 0$.

From these figures, we see that the short time evolution (i.e., for $\Delta t = 1$ s) by the kinetic equations in the mean-field approximation is in agreement with the averages of a detailed numerical solution of the Euler equation. Note that in this period of time, the size of the mixing zone was increased by about 1 cm.

The disagreement of the dashed blue lines with the magenta dotted lines shows that the correct short-time evolution cannot be trivially obtained by the free streaming term alone, i.e., the equation $[\frac{\partial}{\partial t} + v \frac{\partial}{\partial z}] f^{(s)}(z, v, t) \simeq 0$ does not produce the correct evolution even for very short times. This is expected in light of the fact that [as can be seen by integration of Eq. (58) over velocities and summation over $s = 1, 2$] the mean force term is necessary in order to maintain incompressibility.

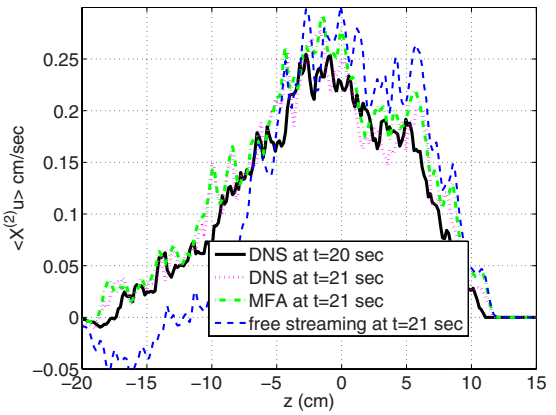

FIG. 8. (Color online) Test of the mean-field approximation.

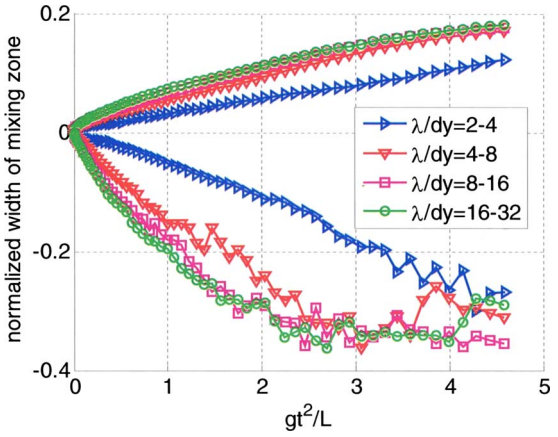

FIG. 9. (Color online) Resolution convergence test.

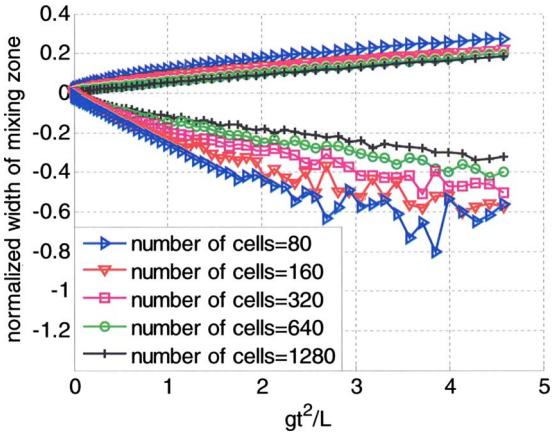

FIG. 10. (Color online) Mode statistics convergence test.

VII. SUMMARY AND DISCUSSION

As is demonstrated in Figs. 3 and 4, the statistics of fluid velocity is not Gaussian. Clearly, not all the effects involved in the RTI mixing are captured by Reynolds average Navier Stokes (RANS) equations for the averaged density, velocity, and energy (or $\langle X^{(s)}\rangle$, $\langle u_z X^{(s)}\rangle$, and $\langle u_z^2 X^{(s)}\rangle$). Closure of the equations by controlled approximations requires equations for higher moments (e.g., kurtosis and flatness [20,32,33]) or equations for the DVPDFs (which contain the information about all moments). This is the approach taken in the present work. Specifically, we have adapted Lundgren's kinetic theoretical approach [11].

The first step in the derivation was the elimination of the pressure (or force) from the fine grain Euler equation by solving the incompressibility condition. The solution [Eq. (8)] relates the force to the velocity and mass density. The combined effect of gravity and density variation introduces two forces: the buoyancy force $\mathbf{F}^b$ defined in Eq. (9) and $\mathbf{F}^{g\rho}$ defined in Eq. (10). The latter is that part of buoyancy force which is determined by the interaction of gravity with the whole density field. In addition, the effect of density variation modifies the nature of the force due to eddies. This is manifested in Eq. (11) by the replacement of the Coulomb Green's function $G_0(\mathbf{r}_1,\mathbf{r}_2)=\frac{1}{4\pi}\frac{1}{|\mathbf{r}_2-\mathbf{r}_1|}$ which governs the pressure (or force) in the case of constant density by a dressed Green's function $G(\mathbf{r},\mathbf{r}')\equiv\{\int G_0(\mathbf{r}-\mathbf{r}'')[\delta^3(\mathbf{r}''-\mathbf{r}')+Q(\mathbf{r}'',\mathbf{r}')]^{-1}d^3\mathbf{r}''\}$. The function $Q(\mathbf{r}'',\mathbf{r}')$ represents the secondary source due to interaction of the bare pressure with density fluctuations.

It is plausible that the dressing of the Green's function effectively screens the source, truncates the range of interaction in the system, and is the origin of the weakness of coupling observed in Fig. 5. This, in turn, is a possible explanation of the capacity of the mean-field approximation in governing the short period time-evolution (Figs. 7 and 8).

The screening assumption reverts the conclusion of Batchelor and Proudman about correlations in constant density turbulence [34] which say: "The fallacy of the old assumption of exponentially small (large separation velocity) cumulants can be ascribed to the action of pressure forces which are local in their effect but which have values determined instantaneously by the whole velocity fields."

To test the screening assumption, one can use a numerical solution of the Euler equation with an additional perturbing force of the form $\varepsilon\rho(\mathbf{r})\frac{1}{4\pi}\frac{\partial}{\partial\mathbf{r}}\frac{1}{|\mathbf{r}-\mathbf{r}_0|}$. The incompressibility condition in this case is as in Eq. (5) but with an additional source term of the form $-\varepsilon\frac{1}{\rho(\mathbf{r})}\delta^3(\mathbf{r}-\mathbf{r}_0)$. The difference between the pressure (or acceleration) in such a run and a reference run with $\varepsilon=0$ reflects the response of the system to the perturbing force. In particular, a pressure difference which falls off faster than $\frac{1}{|\mathbf{r}-\mathbf{r}_0|}$ (which is expected in the case of constant density) would indicate a screening of the perturbing force due to density variation, in contrast with the constant density case analyzed by Batchelor and Proudman [34]. This test requires numerical runs with rich statistics, a task which is left for a future work.

To save computer resources, all the numerical simulations in the present work where limited to two-dimensional runs. We believe that the main conclusions taken from the numerical runs (i.e., the non-Gaussian statistics, the weak coupling, and capacity of the mean-field approximation) are not unique to the two-dimensional case (although the numerical values of parameters such as the rate of expansion of mixing zone may depend on dimensionality [9]). Note that, unlike the constant density case, two-dimensional (2D) Euler equation with density variation does not conserve vorticity, i.e., density variation removes the main difference between 2D turbulence (e.g., Chap. 10 in Ref. [26]) and three-dimensional (3D) turbulence.

Closure of the set of equations (48) beyond the mean-field approximation, requires the extension of the treatment to the equation next to 60 (i.e., the $n=2$ equation). The application of the weak-coupling approximation requires the cluster expansion [similar to Eq. (59)] to all f_n appearing in the $\Delta\mathbf{a}$ term. This derivation as well as the identification of the approximations necessary for closure are not straightforward and are left for a future work.

ACKNOWLEDGMENTS

G.H. acknowledges helpful discussions with D. L. Youngs and D. Livescu.

APPENDIX A: THE MOLECULAR VISCOSITY AND DIFFUSIVITY TERMS

In this appendix, the forms of the additional terms in the fine grain equation (39) due to molecular viscosity and diffusivity are derived. The molecular viscosity term in the Navier-Stokes equation, $-\nu\frac{\partial}{\partial \mathbf{r}_1}\cdot\frac{\partial}{\partial \mathbf{r}_1}\mathbf{u}_1$, may be manipulated in the following way [11]:

$$
\begin{aligned}
&-\nu\left\{\left(\frac{\partial}{\partial \mathbf{r}_1}\cdot\frac{\partial}{\partial \mathbf{r}_1}\mathbf{u}_1\right)\cdot\frac{\partial}{\partial \mathbf{v}_1}[X_1^{(s_1)}\delta^3(\mathbf{u}_1-\mathbf{v}_1)]\right\}\\
&\quad=\nu\frac{\partial}{\partial \mathbf{v}_1}\cdot\left(\lim_{\mathbf{r}_2\to\mathbf{r}_1}\left\{\frac{\partial}{\partial \mathbf{r}_2}\cdot\frac{\partial}{\partial \mathbf{r}_2}[\mathbf{u}_2X_1^{(s_1)}\delta^3(\mathbf{u}_1-\mathbf{v}_1)]\right\}\right)\\
&\quad=\nu\frac{\partial}{\partial \mathbf{v}_1}\cdot\left[\lim_{\mathbf{r}_2\to\mathbf{r}_1}\left(\frac{\partial}{\partial \mathbf{r}_2}\cdot\frac{\partial}{\partial \mathbf{r}_2}\left\{\sum_{s_2=1}^{2}\int d^3\mathbf{v}_2\mathbf{v}_2[X_2^{(s_2)}\delta^3(\mathbf{u}_2-\mathbf{v}_2)X_1^{(s_1)}\delta^3(\mathbf{u}_1-\mathbf{v}_1)]\right\}\right)\right]\\
&\quad=\nu\frac{\partial}{\partial \mathbf{v}_1}\cdot\left(\lim_{\mathbf{r}_2\to\mathbf{r}_1}\left\{\frac{\partial}{\partial \mathbf{r}_2}\cdot\frac{\partial}{\partial \mathbf{r}_2}\left[\sum_{s_2=1}^{2}\int d^3\mathbf{v}_2\mathbf{v}_2F_1^{(s_1)}(\mathbf{r}_1,\mathbf{v}_1,t)F_1^{(s_2)}(\mathbf{r}_2,\mathbf{v}_2,t)\right]\right\}\right).
\end{aligned}
\tag{A1}
$$

Similar treatment to the diffusivity term in the mass conservation equation, $D\frac{\partial}{\partial \mathbf{r}_1}\cdot\frac{\partial}{\partial \mathbf{r}_1}X_1^{(s_1)}$, yields

$$
\begin{aligned}
D\left[\left(\frac{\partial}{\partial \mathbf{r}_1}\cdot\frac{\partial}{\partial \mathbf{r}_1}X_1^{(s_1)}\right)\delta^3(\mathbf{u}_1-\mathbf{v}_1)\right]&=D\left(\lim_{\mathbf{r}_2\to\mathbf{r}_1}\left\{\frac{\partial}{\partial \mathbf{r}_2}\cdot\frac{\partial}{\partial \mathbf{r}_2}[X_2^{(s_2)}\delta^3(\mathbf{u}_1-\mathbf{v}_1)]\right\}\right)\\
&=D\left[\lim_{\mathbf{r}_2\to\mathbf{r}_1}\left(\frac{\partial}{\partial \mathbf{r}_2}\cdot\frac{\partial}{\partial \mathbf{r}_2}\left\{\int d^3\mathbf{v}_2\sum_{s_1=1}^{2}[X_2^{(s_2)}\delta^3(\mathbf{u}_2-\mathbf{v}_2)X_1^{(s_1)}\delta^3(\mathbf{u}_1-\mathbf{v}_1)]\right\}\right)\right]\\
&=D\left(\lim_{\mathbf{r}_2\to\mathbf{r}_1}\left\{\frac{\partial}{\partial \mathbf{r}_2}\cdot\frac{\partial}{\partial \mathbf{r}_2}\left[\int d^3\mathbf{v}_2F_1^{(s_1)}(\mathbf{r}_1,\mathbf{v}_1,t)F_1^{(s_2)}(\mathbf{r}_2,\mathbf{v}_2,t)\right]\right\}\right).
\end{aligned}
\tag{A2}
$$

APPENDIX B: SOME DETAILS OF THE NUMERICAL SCHEME AND CONVERGENCE TESTS

The numerical code LEEOR2D [29] is a two-dimensional finite-difference ALE simulation which uses second-order time integration. The very early stages of the simulation were done in a mode close to Lagrangian, which subsequently changed to Eulerian simulation to avoid Grid distortion.

Two different sets of convergence runs were performed to determine the numerical requirement for the simulation of the RTI evolution, including the self-similar regime. In the figures below, the results of the two sets of convergence runs are presented in terms of the time evolution of the bubbles and spikes fronts. Those are defined as the coordinates at which the y-averaged values of the volume fraction of the light material is 0.04 and 0.96, respectively. The Atwood number was 0.9.

The first convergence test examined the number of cells required per wavelength for a given initial multimode perturbation. Figure 9 presents the results showing that the simulation with 8–16 cells per wavelength is reasonably converged.

The second and more important convergence test addressed the question of statistics required for an adequate simulation of the self-similar regime of RTI. In these runs, the initial perturbation was changed with the resolution so that in all runs, 8–16 cells per wavelength were used and the average amplitude per wavelength was the same. Thus both the wavelengths and the amplitudes decreased with the increased resolution, resulting in a shortening of the transit time to the self-similar regime. Figure 10 presents the normalized width of the mixing zone for increasing resolution. In the runs with higher resolution, the bubble front grows linearly with gt^2 with a proportion coefficient of $\sim$0.04, which is within the range of 0.035–0.05 cited in the literature for 2D simulations (see Refs. 23, 25, 31, 35, 36, 38, and 39 in Ref. [9]).

[1] L. Rayleigh, *Scientific Papers* (Cambridge University Press, Cambridge, England, 1900), Vol. II, p. 200; G. I. Taylor, Proc. R. Soc. London, Ser. A **201**, 192 (1950).
[2] K. I. Read, Physica D **12**, 45 (1984).
[3] G. Dimonte and M. Schneider, Phys. Fluids **12**, 304 (2000).
[4] D. L. Youngs, Physica D **12**, 32 (1984).
[5] D. L. Youngs, Physica D **37**, 270 (1989).
[6] D. L. Youngs, Laser Part. Beams **12**, 725 (1994).
[7] M. B. Schneider, G. Dimonte, and B. Remington, Phys. Rev. Lett. **80**, 3507 (1998).

[8] S. B. Dalziel, P. F. Linden, and D. L. Youngs, J. Fluid Mech. **399**, 1 (1999).
[9] G. Dimonte *et al.*, Phys. Fluids **16**, 1668 (2004).
[10] P. Dimotakis, J. Fluid Mech. **409**, 69 (2000).
[11] T. S. Lundgren, Phys. Fluids **10**, 969 (1967).
[12] N. N. Bogolubov, in *Studies in Statistical Mechanics*, edited by J. de Boer and G. Ulenbeck (North-Holland, Amsterdam, 1962), Vol. I, p. 1.
[13] L. Yu, *Klimontovich Kinetic Theory of Nonideal Gases & Nonideal Plasmas* (Pergamon, New York, 1982).
[14] R. Balescu, *Statistical Mechanics, Matter Out of Equilibrium* (Imperial College Press, London, 1997).
[15] G. Ecker, *Theory of Fully Ionized Plasmas* (Academic, New York, 1972).
[16] N. A. Krall and A. W. Trivelpiece *Principles of Plasma Physics* (McGraw-Hill, New York, 1973).
[17] S. Ichimaru, *Basic Principles of Plasma Physics a Statistical Approach* (Benjamin, New York, 1973).
[18] T. S. Lundgren, Phys. Fluids **12**, 485 (1969).
[19] T. S. Lundgren, *Statistical Models and Turbulence*, Lecture Notes in Physics Vol. 12 (Springer-Verlag, Berlin, 1971), pp. 70–100.
[20] B. Stephen Pope, *Turbulent Flows* (Cambridge University Press, New York, 2000).
[21] D. C. Haworth and S. B. Pope, Phys. Fluids **29**, 387 (1986).
[22] S. B. Pope, Annu. Rev. Fluid Mech. **26**, 23 (1994).
[23] S. B. Pope, Phys. Fluids **6**, 973 (1994).
[24] D. A. Drew, Annu. Rev. Fluid Mech. **15**, 261 (1983).
[25] J. D. Jackson, *Classical Electrodynamic* (Wiley, New York, 1962).
[26] P. A. Davidson, *Turbulence* (Oxford University Press, New York, 2004).
[27] P. Ramaprabhu and M. J. Andrews, J. Fluid Mech. **502**, 233 (2004).
[28] A. M. Polyakov, Phys. Rev. E **52**, 6183 (1995).
[29] D. Ofer, U. Alon, D. Shvarts, R. L. McCrory, and C. P. Verdon, Phys. Plasmas **3**, 3073 (1996).
[30] J. P. Boris, A. M. Landsberg, E. S. Oran, and J. H. Gardner, *LCPPCT—A Flux-Corrected Transport Algorithm for Solving Generalized Continuity Equations*, NRL/MR/6410-93-719 AD-A265 011 (1993).
[31] S. T. Zalesak, J. Comput. Phys. **31**, 335 (1979).
[32] G. K. Batchelor, *The Theory of Homogeneous Turbulence* (Cambridge University Press, New York, 1953).
[33] H. Tennekes and J. L. Lumley, *A First Course in Turbulence* (MIT Press, Cambridge, MA, 1972).
[34] G. K. Batchelor and I. Proudman, Phil. Trans. R. Soc. London, Ser. A **248**, 369 (1956).
[35] G. K. Batchelor, *An Introduction to Fluid Dynamics* (Cambridge University Press, New York, 1988).